MATCH
Communications in Mathematical and in Computer Chemistry

MATCH Commun. Math. Comput. Chem. **89** (2023) 49–71
ISSN: 0340–6253
doi: 10.46793/match.89-1.049A

Mathematical and Kinetic Study of Horiuti-Polanyi Reaction Mechanism for the Methylcyclohexane Dehydrogenation Over Various Pt/Al_2O_3 Catalysts

Muhammad Sarfraz Akram[a,*], Muhammad Rashid Usman[b,c], Faisal Salim Alhumaidan[d]

[a] *Institute of Energy and Environmental Engineering, Faculty of Electrical, Energy and Environmental Engineering, University of the Punjab, Lahore, Pakistan*

[b] *Institute of Chemical Engineering and Technology, Faculty of Chemical and Materials Engineering, University of the Punjab, Lahore, Pakistan*

[c] *Engineering Research Centre, Faculty of Chemical and Materials Engineering, University of the Punjab, Lahore, Pakistan*

[d] *Petroleum Research Center, Kuwait Institute for Scientific Research, Safat, Kuwait*

msakram.ieee@pu.edu.pk, mrusman.icet@pu.edu.pk, fhumaidan@kisr.edu.kw

(Received May 20, 2022)

Abstract

The Horiuti-Polanyi (HP) mechanism has been studied for the methylcyclohexane dehydrogenation reaction over a Pt/Al_2O_3 catalyst. Three HP mechanistic schemes such as competitive, non-competitive, and combined-competitive-non-competitive were used in the kinetic modeling of the experimental data. The loss of first hydrogen atom was regarded as the rate-determining step and the mathematical expressions were developed and fitted against the

*Corresponding author.

data. A FORTRAN routine was employed where 4th order Runge-Kutta method was used to solve the related differential equation and Marquardt algorithm was used for the parametric estimation. A kinetically and statistically best-fit HP kinetic equation was obtained with 87.96 kJ/mol of activation energy. The best-fit kinetic model was tested with five additional Pt-containing Al_2O_3 catalysts and yet again found in good agreement with the experimental data.

1 Introduction

Hydrogenation reactions of alkenes and aromatics are among the oldest and widely studied catalytic reactions [4,13,15,21]. The catalytic chemistry of these hydrogenation reactions was first investigated by Horiuti I, Polanyi M [10]. The researchers conducted a series of experiments for the hydrogenation of ethylene and benzene over Ni and Pt metal surfaces [10]. As a result, they put forward a hydrogenation reaction mechanism which requires successive half hydrogen addition to a hydrocarbon molecule. Their proposed reaction mechanism can be described in the following four steps: a) Dissociative adsorption of hydrogen molecule forming atomic hydrogen adsorbed on a metal surface, b) Non-dissociative adsorption of unsaturated hydrocarbon molecule involving two carbon atoms adsorbed on two adjacent active sites of the metal surface, c) The adsorbed atomic hydrogen reacts with one of the carbon atoms of the adsorbed hydrocarbon to produce the so called half hydrogenated species, d) The reaction further proceeds when another adsorbed atomic hydrogen reacts with the second carbon atom of the adsorbed half hydrogenated intermediate yielding a saturated product that later desorbs from the metal surface.

Since a dehydrogenation reaction is a backward reaction of a corresponding hydrogenation reaction, the mechanism of hydrogenation may well be implemented to a dehydrogenation reaction. Van Trimpont et al. [20] realized this fact and proposed the Horiuti-Polanyi (HP) mechanism to the dehydrogenation reaction of methylcyclohexane (MCH). They reported a competitive HP mechanism which proceeds stepwise with the elimination of six hydrogen atoms forming five reaction intermediates. By competitive, it is meant that the hydrogen and hydrocarbons compete

for the same site. Van Trimpont et al. [20] reasoned that upon ignoring the unstable reaction intermediates, the kinetic rate equations developed based on the above mechanism were expected to be similar to the rate equations developed on the basis of the Langmuir-Hinshelwood-Hougen-Watson (LHHW) mechanism. Van Trimpont et al. [20] therefore did not test the experimental data against their proposed HP scheme. Alhumaidan et al. [3] suggested a non-competitive HP scheme which involved two separate types of sites for the hydrocarbons and hydrogen. They tested only one rate expression developed based on the loss of first hydrogen atom as the rate limiting step. Moreover, they utilized the concept of initial rate kinetics and therefore did not perform a rigorous kinetic analysis. Usman et al. [19] proposed a combined competitive-non-competitive HP reaction mechanism and compared it with the non-competitive HP mechanism. For the in-house synthesized Pt/Al_2O_3 catalyst the non-competitive HP mechanism was found better representative of the data than the competitive-non-competitive HP mechanism. However, they also developed rate equations by assuming only the loss of first hydrogen atom as the rate controlling step, but the kinetic analysis was more rigorous than that used by Alhumaidan et al. [3].

The survey of the literature has revealed that only a very few studies have been carried out on the applications of the HP kinetic mechanism to the dehydrogenation reaction of MCH. Additional studies are therefore required to better understand the HP kinetics for the MCH dehydrogenation. The objective of the present study is to examine and compare the various HP mechanisms discussed above for the dehydrogenation of MCH over Pt containing alumina catalysts. For this purpose, the kinetic equations based on the above mentioned three HP mechanisms were developed and the experimental data of six Pt-loaded alumina catalysts was used to work out the best-fit HP model.

2 Experimental data

The experimental dehydrogenation data of Alhumaidan [2] for Pt loaded six various Al_2O_3 catalysts obtained over an extended range of operating

Table 1. List of the catalysts employed and the ranges of experimental measurements

Catalyst	Assay (wt%)	Type	Impreg. method	S_g (m^2/g)	v_p (cm^3/g)	d_p (Å)	ICP Pt (wt%)	N	T_w (C)	P (bar)	y_{A0}	y_{B0}	y_{C0}	W/F_{A0} x 10^{-5} (s g-cat/mol)
CAT-A	1.0Pt/ γ-Al_2O_3	Com	N/A	302.3	0.52	67.2	0.86	130	340– 450	1.0– 9.0	0.105– 1.0	0	0.0– 0.895	0.306– 1.225
CAT-B	0.5Pt/ γ-Al_2O_3	Com	N/A	124.6	0.35	110.3	0.42	36	380– 450	1.0– 9.0	0.105– 1.0	0	0.0– 0.895	0.306– 1.225
CAT-C	0.3Pt/ γ-Al_2O_3	IH	Wet	220	0.62	70	0.24	36	380– 450	1.0– 9.0	0.105– 1.0	0	0.0– 0.895	0.306– 1.225
CAT-D	0.3Pt-0.3Re/ γ-Al_2O_3	IH	Wet-Co	220	0.62	70	0.28	36	380– 450	1.0– 9.0	0.105– 1.0	0	0.0– 0.895	0.306– 1.225
CAT-E	0.3Pt-0.3Pd/ γ-Al_2O_3	IH	Wet-Co	220	0.62	70	0.26	36	380– 450	1.0– 9.0	0.105– 1.0	0	0.0– 0.895	0.306– 1.225
CAT-F	0.3Pt-0.3Re/ γ-Al_2O_3	IH	Wet-Seq	220	0.62	70	0.25	24	380– 450	1.0– 9.0	0.105– 1.0	0	0.0– 0.895	0.306– 1.225

Com=commercial:IH=in-house:S_g=N_2-BET surface area:v_p=pore volume:d_p=median pore diameter:N=total number of experimental data points:T_w=wall temperature:y_{A0},y_{B0},y_{C0}=initial mole fraction of MCH, toluene and hydrogen in the gas phase:W=weight of catalyst:F_{A0}=initial molar flowrate of MCH

conditions was exploited to perform the kinetic modeling of the dehydrogenation reaction. The particulars of the catalysts and the experimental operating conditions used in the study are shown in Table 1. The experiments were performed in a laboratory fixed bed reactor and the reaction products were condensed and analyzed by a gas chromatograph. Additional detail about the experimental apparatus and the procedure can be found in Alhumaidan [2].

3 Method of kinetic analysis

The laboratory dehydrogenation reactor was considered a plug flow reactor and was described by the performance equation shown below:

$$\frac{dX_A}{d\left(\frac{W}{F_{A0}}\right)} = (-r_A)' \tag{1}$$

where, X_A = fractional conversion of MCH, W = weight of catalyst (g), F_{A0} = initial molar flowrate of MCH (mol/s) and $(-r_A)'$ = rate of the dehydrogenation reaction (mol/s g-cat).

The following form of the Arrhenius equation was employed to observe the effect of temperature dependency on the rate of the reaction:

$$k = k_r exp\left[Arr\left(1 - \frac{T_r}{T}\right)\right] \tag{2}$$

$$Arr = \frac{E_a}{RT_r} \tag{3}$$

where, k_r = rate constant at reference temperature T_r, Arr = dimensionless activation energy or Arrhenius number, Ea = activation energy (kJ/mol), R = universal gas constant (kJ/mol K), T = reaction temperature (K) and T_r = average reaction temperature of all the experimental temperatures (K) [12].

As the experimental data was taken under integral conditions and usually high conversions close to the equilibrium conversions were obtained, reversibility effect was also included in the rate equations. The following

experimentally found equilibrium constant after Schildhauer et al. [16] was employed to incorporate the reversibility effect:

$$K = 3600exp\left[\frac{-217650}{R}\left(\frac{1}{T} - \frac{1}{650}\right)\right] \tag{4}$$

where, K = equilibrium constant of the MCH dehydrogenation reaction (bar^3), R is in J/(mol K), and T is in K.

In obtaining the experimental data, four experimental runs were performed in a sequence, consuming a total of 415 min, before reclaiming the catalyst activity. The effect of this short-term deactivation was therefore also included in the rate models. The following deactivation term was employed with the developed rate models:

$$(-r_A)' = (-r_A)(1 - k_d t_d) \tag{5}$$

where, k_d is the deactivation rate constant in day^{-1} and is the deactivation time in day.

Eqs. 1-5 together with a proposed rate equation were solved and fitted against the experimental data using a FORTRAN routine. The FORTRAN program employed the 4th order Runge-Kutta method and Marquardt algorithm to solve the differential equation and to optimize the regression parameters. The sum of the squares of the errors (SSE), Eq. 6, for the experimental and model conversions was taken as the objective function to be minimized. All the developed kinetic rate equations were tested this way and the best-fit rate equation was identified. The first discrimination among the kinetic rate equations was done on the basis of SSE value, F-value (Eq. 6 and Eq. 8), and kinetic validity of the parameters, i.e., the parameters must be non-negative.

$$Obj_{fn} = SSE = \sum_{i}^{N}[(X_{A,obs})_i - (X_{A,mod})_i]^2 \tag{6}$$

$$SSM = \sum_{i=1}^{i=N}[(X_{A,obs})_i - \overline{X}_A]^2 \tag{7}$$

$$F = \left(\frac{SSM - SSE}{m-1}\right) \cdot \left(\frac{SSE}{N-m}\right)^{-1} \tag{8}$$

After the first discrimination, the selected kinetic models were subjected to the second discrimination by giving the temperature dependency to the adsorption equilibrium constants [19, 20]. Additionally, the rival models were compared by the percentage error and AdjR^2 as calculated using Eq. 9 and Eq. 10, respectively.

$$\%error = \frac{100}{N} \sum_{i}^{N} \left(\left| \frac{(X_{A,obs})_i - (X_{A,\mathrm{mod}})_i}{(X_{A,obs})_i} \right| \right) \tag{9}$$

$$AdjR^2 = 1 - \frac{SSE(N-1)}{SSM(N-m-1)} \tag{10}$$

The kinetic model with the minimum SSE (and relatively high F-value) was regarded as the best-fit kinetic model to the experimental data. A schematic diagram explaining the above procedure is shown Figure 1.

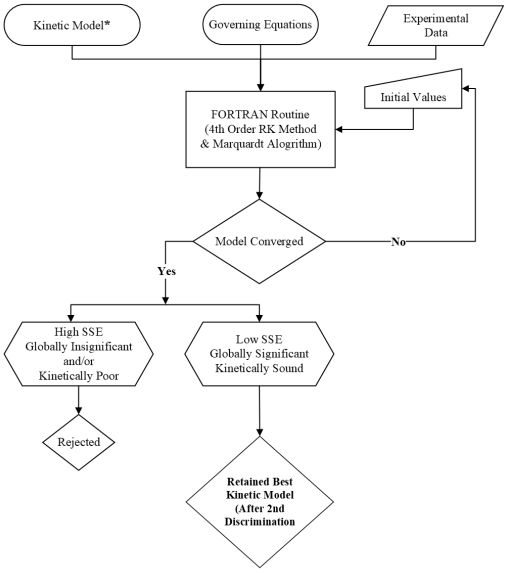

Figure 1. Schematic diagram of computer procedure to obtain best kinetic model

4 Results and discussion

4.1 HP kinetic schemes and the development of kinetic model equations

Three HP kinetic schemes were employed to model the experimental data. Scheme-I, shown in Table 2, is based on the competitive HP mechanism, i.e., both hydrogen and hydrocarbons look for the identical kind of active sites [7, 20]. This scheme is proposed by Van Trimpont et al. [20] and contains only one kind of active sites. Table 3 shows Scheme-II that is based on the non-competitive Horiuti-Polanyi mechanism. It contains two different types of active sites and hydrogen and hydrocarbons are adsorbed on the separate kinds of sites. Following Van Trimpont et al. [20], Alhumaidan et al. [3] laid down the reaction steps for Scheme-II that is different to Scheme-I only in hydrogen adsorption on a different type of site. Scheme-III, shown in Table 4, is based on the combined-competitive-non-competitive HP mechanism and combines the concept of Scheme-I and Scheme-II. It contains two different types of sites and both of these sites are available for hydrogen. The elementary steps of Scheme-III were outlined by Usman et al. [19].

Table 2. Scheme-I: Dual-site reaction mechanism, evolution of atomic hydrogen proposed by Van Trimpont et al. [20]

Mechanistic step	Step no.
$MCH + s \rightleftharpoons MCH \cdot s$	(I)
$MCH \cdot s + s \rightleftharpoons MCH1 \cdot s + H \cdot s$	(II)
$MCH1 \cdot s + s \rightleftharpoons MCHe \cdot s + H \cdot s$	(III)
$MCHe \cdot s + s \rightleftharpoons MCH2 \cdot s + H \cdot s$	(IV)
$MCH2 \cdot s + s \rightleftharpoons MCHde \cdot s + H \cdot s$	(V)
$MCHde \cdot s + s \rightleftharpoons MCH3 \cdot s + H \cdot s$	(VI)
$MCH3 \cdot s + s \rightleftharpoons Tol \cdot s + H \cdot s$	(VII)
$Tol \cdot s \rightleftharpoons Tol + s$	(VIII)
$2H \cdot s \rightleftharpoons H_2 + 2s$	(IX)

s = empty or active site on catalyst

Table 3. Scheme-II: Non-competitive scheme outlined by Alhumaidan et al. [3]

Mechanistic step	Step no.
$MCH + s \rightleftharpoons MCH \cdot s$	(I)
$MCH \cdot s + s^* \rightleftharpoons MCH1 \cdot s + H \cdot s^*$	(II)
$MCH1 \cdot s + s^* \rightleftharpoons MCHe \cdot s + H \cdot s^*$	(III)
$MCHe \cdot s + s^* \rightleftharpoons MCH2 \cdot s + H \cdot s^*$	(IV)
$MCH2 \cdot s + s^* \rightleftharpoons MCHde \cdot s + H \cdot s^*$	(V)
$MCHde \cdot s + s^* \rightleftharpoons MCH3 \cdot s + H \cdot s^*$	(VI)
$MCH3 \cdot s + s^* \rightleftharpoons Tol \cdot s + H \cdot s^*$	(VII)
$Tol \cdot s \rightleftharpoons Tol + s$	(VIII)
$2H \cdot s^* \rightleftharpoons H_2 + 2s^*$	(IX)

s^* = hydrogen-only empty or active site on catalyst

Table 4. Scheme-III Reaction scheme for the competitive-non-competitive Horiuti-Polanyi mechanism proposed by Usman et al. [19]

Mechanistic step	Step no.
$MCH + s \rightleftharpoons MCH \cdot s$	(I)
$MCH \cdot s + s \rightleftharpoons MCH1 \cdot s + H \cdot s$	(II)
$MCH \cdot s + s^* \rightleftharpoons MCH1 \cdot s + H \cdot s^*$	(III)
$MCH1 \cdot s + s \rightleftharpoons MCHe \cdot s + H \cdot s$	(IV)
$MCH1 \cdot s + s^* \rightleftharpoons MCHe \cdot s + H \cdot s^*$	(V)
$MCHe \cdot s + s \rightleftharpoons MCH2 \cdot s + H \cdot s$	(VI)
$MCHe \cdot s + s^* \rightleftharpoons MCH2 \cdot s + H \cdot s^*$	(VII)
$MCH2 \cdot s + s \rightleftharpoons MCHde \cdot s + H \cdot s$	(VIII)
$MCH2 \cdot s + s^* \rightleftharpoons MCHde \cdot s + H \cdot s^*$	(IX)
$MCHde \cdot s + s \rightleftharpoons MCH3 \cdot s + H \cdot s$	(X)
$MCHde \cdot s + s^* \rightleftharpoons MCH3 \cdot s + H \cdot s^*$	(XI)
$MCH3 \cdot s + s \rightleftharpoons Tol \cdot s + H \cdot s$	(XII)
$MCH3 \cdot s + s^* \rightleftharpoons Tol \cdot s + H \cdot s^*$	(XIII)
$Tol \cdot s \rightleftharpoons Tol + s$	(XIV)
$2H \cdot s \rightleftharpoons H_2 + 2s$	(XV)
$2H \cdot s^* \rightleftharpoons H_2 + 2s^*$	(XVI)

Table 5. Kinetic equations developed based on HP mechanism (Usman et al.) [19]

Model name	Kinetic equation
HPC-0 (Competitive HP)	$(-r_A) = \frac{kK_A p_A \left(1-\frac{p_B {p_C}^3}{K p_A}\right)}{(1+K_A p_A+K_B p_B+\sqrt{K_C p_C})^2}$
HPNC-0 (Non-competitive HP)	$(-r_A) = \frac{kK_A p_A \left(1-\frac{p_B {p_C}^3}{K p_A}\right)}{(1+K_A p_A+K_B p_B)(1+\sqrt{K^*_C p_C})}$
HPCCNC-0 (Combined Competitive-non-competitive HP)	$(-r_A) = \frac{kK_A p_A \left(1-\frac{p_B {p_C}^3}{K p_A}\right)}{(1+K_A p_A+K_B p_B+\sqrt{K_C p_C})(1+\sqrt{K^*_C p_C})}$

K=equilibrium constant of the MCH dehydrogenation reaction, bar^3: k=rate constant for the MCH dehydrogenation reaction: K_A=adsorption equilibrium constant of MCH, bar^{-1}: K_B=adsorption equilibrium constant of toluene, bar^{-1}: K_C=adsorption equilibrium constant of hydrogen, bar^{-1}: K^*_C=adsorption equilibrium constant of hydrogen adsorbed on site s*, bar^{-1}: p_A=partial pressure of MCH, bar: p_B=partial pressure of toluene, bar: p_C=partial pressure of hydrogen, bar$^{1/2}$

For each HP scheme a kinetic model was developed assuming the loss of first hydrogen atom (the second step of each scheme) as the rate controlling step. The reason for this choice lies in the fact that majority of the literature [1,3,6,9,17,19,20] related to the dehydrogenation of methylcyclohexane, have found the first surface reaction as the most difficult reaction to occur. Table 5 shows the three kinetic model equations obtained for the three HP kinetic schemes discussed above. In the development of each of the three rate equations, for the simplification (i.e., to have fewer parameters), the surface coverage of all the intermediate species was considered negligible. The model equation (HPNC-0) based on Scheme-II is developed by Alhumaidan et al. [3] while the kinetic equation (HPCCNC-0) based on Scheme-III is developed by Usman et al. [19]. The kinetic rate model (HPC-0) based on Scheme-I is derived in the present study and for the interested reader, the derivation steps are provided in Table 6.

Each model equation given in Table 5 returned additional (sub) kinetic models by removing one or more denominator terms [19]. For example,

based on the kinetic model developed using Scheme-II, 31 additional models were produced. In this way a total of 168 kinetic models were developed. It is important to mention here that the mathematical expressions for a few kinetic models were found similar though developed on the basis of different kinetic schemes.

Table 6. Derivation of kinetic model for Scheme-II using Step-II as the rate determining step

---

From Step-I:

$$(-r_A) = 0 = k_1 p_{MCH} C_s - k_{-1} C_{MCH\cdot s} \rightarrow C_{MCH\cdot s} = K_1 p_{MCH} C_s \quad (A.1)$$

From Step-II (RDS):

$$(-r_A) = k_2 C_{MCH\cdot s} C_s - k_{-2} C_{MCH1} C_{H\cdot s} \quad (A.2)$$

From-III:

$$(-r_A) = 0 = k_3 C_{MCH1\cdot s} C_s - k_{-3} C_{MCHe\cdot s} C_{H\cdot s} \rightarrow$$

$$C_{MCH1\cdot s} = \frac{C_{MCHe\cdot s} C_{H\cdot s}}{K_3 C_s} \quad (A.3)$$

From-IV:

$$(-r_A) = 0 = k_4 C_{MCHe\cdot s} C_s - k_{-4} C_{MCH2\cdot s} C_{H\cdot s} \rightarrow$$

$$C_{MCHe\cdot s} = \frac{C_{MCH2\cdot s} C_{H\cdot s}}{K_4 C_s} \quad (A.4)$$

From-V:

$$(-r_A) = 0 = k_5 C_{MCH2\cdot s} C_s - k_{-5} C_{MCHde\cdot s} C_{H\cdot s} \rightarrow$$

$$C_{MCH2\cdot s} = \frac{C_{MCHde\cdot s} C_{H\cdot s}}{K_5 C_s} \quad (A.5)$$

From-VI:

$$(-r_A) = 0 = k_6 C_{MCHde\cdot s} C_s - k_{-6} C_{MCH3\cdot s} C_{H\cdot s} \rightarrow$$

$$C_{MCHde\cdot s} = \frac{C_{MCH3\cdot s} C_{H\cdot s}}{K_6 C_s} \quad (A.6)$$

From-VII:

$$(-r_A) = 0 = k_7 C_{MCH3\cdot s} C_s - k_{-7} C_{Tol\cdot s} C_{H\cdot s} \rightarrow$$

$$C_{MCH3\cdot s} = \frac{C_{B\cdot s} C_{H\cdot s}}{K_7 C_s} \quad (A.7)$$

From-VIII:

$$(-r_A) = 0 = k_8 C_{Tol\cdot s} - k_{-8} p_{Tol} C_s \rightarrow C_{Tol\cdot s} = K_8 p_{Tol} C_s \qquad (A.8)$$

From-IX:

$$(-r_A) = 0 = k_9 C_{H\cdot s}^2 - k_{-9} p_{H2} C_s \rightarrow C_{H\cdot s} = \sqrt{K_9 p_{H2} C_s^2} \qquad (A.9)$$

$$C_{A\cdot s} = K_A p_A C_s \qquad (A.1)$$

$$C_{B\cdot s} = K_B p_B C_s \qquad (A.8)$$

$$C_{H\cdot s} = \sqrt{K_C p_C C_s^2} \qquad (A.9)$$

From Step-II (RDS):

$$(-r_A) = k_2 C_{MCH\cdot s} C_s - k_{-2} C_{MCH1} C_{H\cdot s} \qquad (A.2)$$

$$C_{MCH1\cdot s} = \frac{C_{H\cdot s}}{K_3 C_s} \frac{C_{H\cdot s}}{K_4 C_s} \frac{C_{H\cdot s}}{K_5 C_s} \frac{C_{H\cdot s}}{K_6 C_s} \frac{K_B p_B C_s C_{H\cdot s}}{K_7 C_s}$$

$$C_{MCH1\cdot s} = \frac{K_C^3 p_C^3 C_s^2}{K_3} \frac{1}{K_4} \frac{1}{K_5} \frac{1}{K_6} \frac{K_B p_B}{K_7}$$

$$(-r_A) = k_2 K_A p_A C_s^2 - k_{-2} \frac{K_C^3 p_C^3 C_s^2}{K_3} \frac{1}{K_4} \frac{1}{K_5} \frac{1}{K_6} \frac{K_B p_B}{K_7}$$

$$(-r_A) = k_2 K_A C_s^2 \left(p_A - \frac{p_B p_C^3}{K} \right)$$

$$C_T = C_s + K_A p_A C_s + K_B p_B C_s + \sqrt{K_C p_C} C_s$$

$$C_s = \frac{C_T}{1 + K_A p_A + K_B p_B + \sqrt{K_C p_C}}$$

$$(-r_A) = \frac{k K_A p_A \left(1 - \frac{p_B p_C^3}{K p_A} \right)}{(1 + K_A p_A + K_B p_B + \sqrt{K_C p_C})^2}$$

4.2 Kinetic analysis with the experimental data of CAT-A

For the first discrimination, all the developed kinetic model equations mentioned above were tested with CAT-A for which an extensive set of experimental data (of 130 runs) was available. Based on the low value of SSE and a rather high value of F, four kinetic models as shown in Table 7, were

Table 7. Kinetic models with their regression results retained after the first discrimination

Kinetic model label and equation	Results
HPCCNC-52 (HPNC-26) m=6 $(-r_A) = \frac{kK_A p_A \left(1 - \frac{p_B p_C{}^3}{K p_A}\right)}{1+K_B p_B + K_A p_A \sqrt{K_C^* p_C} + K_B p_B \sqrt{K_C^* p_C}}$	SSE 0.281 F-value 638.5 %error 7.64 AdjR^2 0.961 NPs 0 Ea 73.54
HPCCNC-72 (HPNC-31) m=6 $(-r_A) = \frac{kK_A p_A \left(1 - \frac{p_B p_C{}^3}{K p_A}\right)}{1+K_A p_A + K_B p_B + K_A p_A \sqrt{K_C^* p_C} + K_B p_B \sqrt{K_C^* p_C}}$	SSE 0.282 F-value 636.0 %error 7.750 AdjR^2 0.961 NPs 0 Ea 73.08
HPCCNC-91 (HPNC-30) m=6 $(-r_A) = \frac{kK_A p_A \left(1 - \frac{p_B p_C{}^3}{K p_A}\right)}{1+K_B p_B + \sqrt{K_C^* p_C} + K_A p_A \sqrt{K_C^* p_C} + K_B p_B \sqrt{K_C^* p_C}}$	SSE 0.281 F-value 638.3 %error 7.636 AdjR^2 0.960 NPs 0 Ea 73.72
HPCCNC-106 (HPNC-0) m=6 $(-r_A) = \frac{kK_A p_A \left(1 - \frac{p_B p_C{}^3}{K p_A}\right)}{1+K_A p_A + K_B p_B + \sqrt{K_C^* p_C} + K_A p_A \sqrt{K_C^* p_C} + K_B p_B \sqrt{K_C^* p_C}}$	SSE 0.282 F-value 635.6 %error 7.752 AdjR^2 0.960 NPs 0 Ea 73.19

Model label in parentheses shows the equivalent model, %error is the error defined in Eq. 9, and NPs is number of negative parameters.

retained after the first discrimination. These retained models are based on either Scheme-II or Scheme-III and as shown in Table 7 provide virtually the same fit. In each case, the objective function (SSE) is around 0.28 and a relatively high F value close to 635 is obtained. Moreover, each selected model has inhibition terms that contain K_A, K_B, and K^*_C (but not K_C) suggesting the occurrence of methylcyclohexane, toluene, and hydrogen adsorbed on sites different to the hydrocarbon sites might inhibit the rate. In the second discrimination, for the above four kinetic models, the adsorption equilibrium constants were given the temperature dependency similar to the one shown in Eq. 2. The results of the second discrimination are shown in Table 8.

Table 8. Results of the second discrimination among the rival models

HPCCNC-52	SSE	0.281
(HPNC-26)	F-value	638.5
m = 6	%error	7.639
$(-r_A) = \frac{kK_{AP_A}\left(1-\frac{p_B p_C{}^3}{K_{P_A}}\right)}{(1+K_{BP_B}+K_{AP_A}\sqrt{K^*_C p_C}+K_{BP_B}\sqrt{K^*_C p_C})}$	$Adj R^2$	0.961
	NPs	0
	Ea	73.54
HPCCNC-52-1	SSE	0.296
m = 7	F-value	499.7
$(-r_A) = \frac{kK_{AP_A}\left(1-\frac{p_B p_C{}^3}{K_{P_A}}\right)}{(1+K_{BP_B}+K_{AP_A}\sqrt{K^*_C p_C}+K_{BP_B}\sqrt{K^*_C p_C})}$	%error	7.555
$fn(T) = K_A$	$Adj R^2$	0.958
	NPs	0
	Ea	71.93
HPCCNC-52-2	SSE	0.28
m = 7	F-value	529.8
$(-r_A) = \frac{kK_{AP_A}\left(1-\frac{p_B p_C{}^3}{K_{P_A}}\right)}{(1+K_{BP_B}+K_{AP_A}\sqrt{K^*_C p_C}+K_{BP_B}\sqrt{K^*_C p_C})}$	%error	7.622
$fn(T) = K_B$	$Adj R^2$	0.962
	NPs	0
	Ea	80.24

The kinetic model, HPCCNC-72 which is equivalent to HPNC-31 when subjected to temperature dependency of parameter produced the lowest value of the objective function. The objective function, SSE, decreased

HPCCNC-52-3	SSE	0.279
m = 7	F-value	532.9
$(-r_A) = \frac{kK_A p_A \left(1-\frac{p_B p_C{}^3}{K p_A}\right)}{(1+K_B p_B+K_A p_A\sqrt{K_C^* p_C}+K_B p_B\sqrt{K_C^* p_C})}$	%error	7.317
	$AdjR^2$	0.961
$fn(T) = \sqrt{K_C^*}$	NPs	0
	Ea	83.18
HPCCNC-72	SSE	0.282
(HPNC-31)	F-value	636
m = 6	%error	7.748
$(-r_A) = \frac{kK_A p_A \left(1-\frac{p_B p_C{}^3}{K p_A}\right)}{(1+K_A p_A+K_B p_B+K_A p_A\sqrt{K_C^* p_C}+K_B p_B\sqrt{K_C^* p_C})}$	$AdjR^2$	0.961
	NPs	0
	Ea	73.08
HPCCNC-72-1	SSE	0.281
m = 7	F-value	528.5
$(-r_A) = \frac{kK_A p_A \left(1-\frac{p_B p_C{}^3}{K p_A}\right)}{(1+K_A p_A+K_B p_B+K_A p_A\sqrt{K_C^* p_C}+K_B p_B\sqrt{K_C^* p_C})}$	%error	7.679
	$AdjR^2$	0.96
$fn(T) = K_A$	NPs	0
	Ea	73.22
HPCCNC-72-2	SSE	0.28
m = 7	F-value	529.6
$(-r_A) = \frac{kK_A p_A \left(1-\frac{p_B p_C{}^3}{K p_A}\right)}{(1+K_A p_A+K_B p_B+K_A p_A\sqrt{K_C^* p_C}+K_B p_B\sqrt{K_C^* p_C})}$	%error	7.694
	$AdjR^2$	0.961
$fn(T) = K_B$	NPs	0
	Ea	74.22
HPCCNC-72-3	SSE	0.265
m = 7	F-value	560.8
$(-r_A) = \frac{kK_A p_A \left(1-\frac{p_B p_C{}^3}{K p_A}\right)}{(1+K_A p_A+K_B p_B+K_A p_A\sqrt{K_C^* p_C}+K_B p_B\sqrt{K_C^* p_C})}$	%error	7.275
	$AdjR^2$	0.963
$fn(T) = \sqrt{K_C^*}$	NPs	0
	Ea	80.64

HPCCNC-91	SSE	0.281
(HPNC-30)	F-value	638.3
m = 6	%error	7.636
$(-r_A) =$	$AdjR^2$	0.961
$\frac{kK_Ap_A\left(1-\frac{p_Bp_C{}^3}{Kp_A}\right)}{(1+K_Bp_B+\sqrt{K_C^*p_C}+K_Ap_A\sqrt{K_C^*p_C}+K_Bp_B\sqrt{K_C^*p_C})}$	NPs	0
	Ea	73.72
HPCCNC-91-1	SSE	0.285
m = 7	F-value	520.4
$(-r_A) =$	%error	7.638
$\frac{kK_Ap_A\left(1-\frac{p_Bp_C{}^3}{Kp_A}\right)}{(1+K_Bp_B+\sqrt{K_C^*p_C}+K_Ap_A\sqrt{K_C^*p_C}+K_Bp_B\sqrt{K_C^*p_C})}$	$AdjR^2$	0.966
$fn(T) = K_A$	NPs	0
	Ea	76.93
HPCCNC-91-2	SSE	0.28
m = 7	F-value	531.1
$(-r_A) =$	%error	7.605
$\frac{kK_Ap_A\left(1-\frac{p_Bp_C{}^3}{Kp_A}\right)}{(1+K_Bp_B+\sqrt{K_C^*p_C}+K_Ap_A\sqrt{K_C^*p_C}+K_Bp_B\sqrt{K_C^*p_C})}$	$AdjR^2$	0.961
$fn(T) = K_B$	NPs	0
	Ea	77.99
HPCCNC-91-3	SSE	0.282
m = 7	F-value	527
$(-r_A) =$	%error	7.646
$\frac{kK_Ap_A\left(1-\frac{p_Bp_C{}^3}{Kp_A}\right)}{(1+K_Bp_B+\sqrt{K_C^*p_C}+K_Ap_A\sqrt{K_C^*p_C}+K_Bp_B\sqrt{K_C^*p_C})}$	$AdjR^2$	0.96
$fn(T) = \sqrt{K_C^*}$	NPs	0
	Ea (kJ/mol)	72.96
HPCCNC-106	SSE	0.282
(HPNC-0)	F-value	635.6
m = 6	%error	7.751
$(-r_A) =$	$AdjR^2$	0.961
$\frac{kK_Ap_A\left(1-\frac{p_Bp_C{}^3}{Kp_A}\right)}{(1+K_Ap_A+K_Bp_B+\sqrt{K_C^*p_C}+K_Ap_A\sqrt{K_C^*p_C}+K_Bp_B\sqrt{K_C^*p_C})}$	NPs	0
	Ea	73.19

HPCCNC-106-1	SSE	0.283
m = 7	F-value	525
$(-r_A) =$	%error	7.747
$\frac{kK_Ap_A\left(1-\frac{p_Bp_C{}^3}{Kp_A}\right)}{(1+K_Ap_A+K_Bp_B+\sqrt{K_C^*p_C}+K_Ap_A\sqrt{K_C^*p_C}+K_Bp_B\sqrt{K_C^*p_C})}$	$AdjR^2$	0.96
	NPs	0
$fn(T) = K_A$	Ea	72.12
HPCCNC-106-2	SSE	0.283
m = 7	F-value	525.3
$(-r_A) =$	%error	7.748
$\frac{kK_Ap_A\left(1-\frac{p_Bp_C{}^3}{Kp_A}\right)}{(1+K_Ap_A+K_Bp_B+\sqrt{K_C^*p_C}+K_Ap_A\sqrt{K_C^*p_C}+K_Bp_B\sqrt{K_C^*p_C})}$	$AdjR^2$	0.96
	NPs	0
$fn(T) = K_B$	Ea	73.02
HPCCNC-106-3	SSE	0.313
m = 7	F-value	471.8
$(-r_A) =$	%error	8.372
$\frac{kK_Ap_A\left(1-\frac{p_Bp_C{}^3}{Kp_A}\right)}{(1+K_Ap_A+K_Bp_B+\sqrt{K_C^*p_C}+K_Ap_A\sqrt{K_C^*p_C}+K_Bp_B\sqrt{K_C^*p_C})}$	$AdjR^2$	0.96
	NPs	0
$fn(T) = \sqrt{K_C^*}$	Ea	113

Model label in parentheses shows the equivalent model, m is number of parameters of model, SSE is the sum of squares of the errors, %error is the error defined in Eq. 9, and NPs is number of negative parameters.

from 0.282 for HPCCNC-72 model to 0.265 for CCNC-72-3 model. Moreover, a relatively high value of F statistics, i.e., 560.8 shows adequate global significance of the model. All the parameters were found kinetically sound and the activation energy of 80.65 kJ/mol was obtained. The kinetic model HPCCNC-72-3 was therefore regarded as the best-fit model for the experimental data of CAT-A. The detailed results of regression for the best-fit model are shown in Table 9, whereas a plot of experimental and predicted conversions along with a plot of residuals is shown in Figure 2.

For a Pt/Al_2O_3 catalyst, a series of activation energy is reported in the literature. The value ranges from 17.90 kJ/mol by El-Sawi [8] to 220.7 kJ/mol by Maria et al. [14]. A value of 80.65 kJ/mol, found in the

present study, is in accordance with Jossens and Petersen [11] who reported 71.13 kJ/mol over the Pt/Al_2O_3 used in their work. Other studies in the literature have also found the activation energy relatively close to the above value. For example, Usman et al., [18] while working on a commercial dehydrogenation catalyst had obtained activation energy of 100.1 kJ/mol.

Table 9. Detailed results of regression with the best-fit model for CAT-A

Kinetic model equation					
$(-r_A) = \frac{kK_A p_A\left(1-\frac{p_B p_C{}^3}{K p_A}\right)}{1+K_A p_A+K_B p_B+K_A p_A\sqrt{K_C^* p_C}+K_B p_B\sqrt{K_C^* p_C}}(1-k_d t_d)$					
$k = k_r exp\left[Arr\left(1-\frac{617.39}{T}\right)\right]$					
$A_{rr} = \frac{Ea}{617.39R}$					
$\sqrt{K_C^*} = K_{Cr}^* exp[H_C^*\left(1-\frac{617.39}{T}\right)]$					
$\mathrm{H}^*{}_C = \frac{\Delta h_C^*}{617.39R}$					
Overall statistical results					
N	m	$AdjR^2$	SSE	F	%error
130	7	0.9627	0.2653	560.81	7.2750
Kinetics parameters with their statistics					
Parameter	Value	Unit	Parameter	Value	Unit
$K_r \times 10^5$	19.14	$molg-cat^{-1}s^{-1}$	$K^*{}_{Cr}$	4.249	$bar^{1/2}$
Arr	15.71	–	$H^*{}_C$	1.463	–
(Ea)	(80.65)	$(kJmol^{-1})$	(Δh_C^*)	(7.512)	$(kJmol^{-1})$
K_A	372.4	bar^{-1}	k_d	1.322	day^{-1}
K_B	374.1	bar^{-1}			

$H^*{}_C$=dimensionless heat of adsorption for hydrogen: $\Delta h^*{}_C$=heat of adsorption for hydrogen: K_{Cr}=adsorption equilibrium constant of hydrogen at T_r: $K^*{}_{Cr}$=adsorption equilibrium constant of hydrogen adsorbed on site s* at T_r: k_r=rate constant at reference temperature T_r

The value is supported by Campbell [5] while working the liquid phase dehydrogenation of methylcyclohexane. Tsakiris [17] for one of his Pt-impregnated alumina catalysts reported the activation energy as 60.0 kJ/mol.

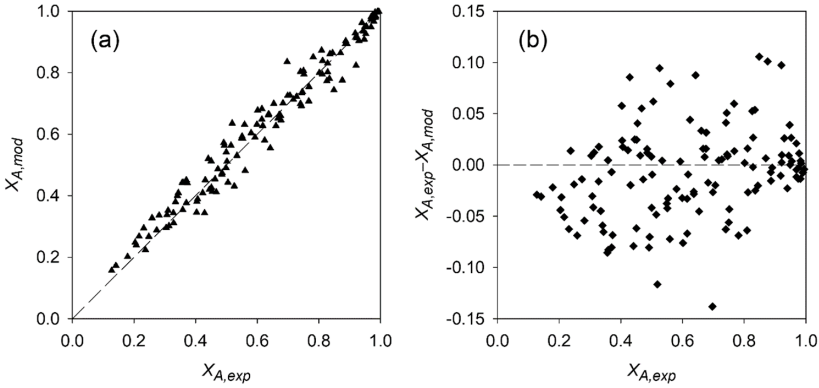

Figure 2. Quality of fitting experimental conversions and predicted conversions obtained with the best-fit model (HPCCNC-72-3 or HPNC-31-3) for CAT-A. a) Parity diagram between experimental and observed conversions, b) Plot of residuals.

4.3 Kinetic analysis with the experimental data of CAT-B, CAT-C, CAT-D, CAT-E, and CAT-F

The best-fit kinetic model, HPCCNC-72-3 (with temperature dependency of in HPCCNC-72), was further employed to fit the experimental data of additional five Pt-containing alumina catalysts. This is done to check the applicability of the retained model to the experimental data of other Pt loaded Al_2O_3 catalysts. The results of the fitting are shown in Table 10 and the parity plots of experimental and model conversions are prepared as shown in Figure 3. In each case SSE value is found less than 0.12 and large F-values are obtained which show that the form of the best-fit kinetic model found in the present study has the ability to fit the data of several other, if not all, Pt-loaded alumina catalysts.

Table 10. Results of regression with the best-fit model for CAT-B, -C, -D, -E, and -F

Model		CAT-B (N = 36)	CAT-C (N = 36)	CAT-D (N = 36)	CAT-E (N = 36)	CAT-F (N = 24)
HPCCNC-72-3	SSE	0.076	0.067	0.057	0.113	0.018
(HPNC-31-3)	F-value	80.98	84.59	96.65	48.52	116.8
m = 7	%error	5.374	4.456	4.156	6.126	3.036
	AdjR^2	0.93	0.932	0.94	0.887	0.966
	NPs	0	0	0	0	0
	Ea (kJ/mol)	113.2	179.4	87.86	77.99	234.2

Model label in parentheses shows the equivalent model, %error is the error defined in Eq. 9, and NPs is number of negative parameters.

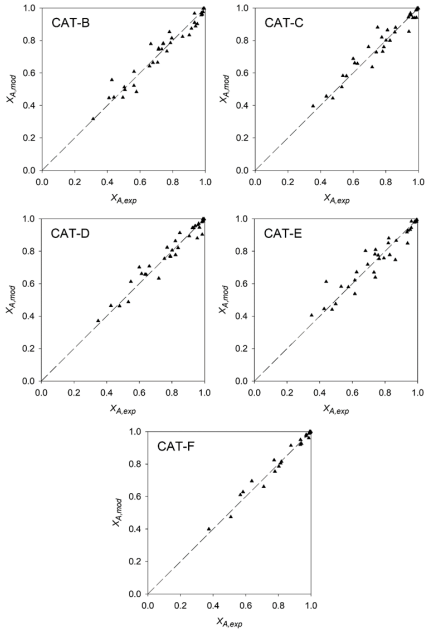

Figure 3. Quality of fitting experimental conversions and predicted conversions obtained with the best-fit model (HPCCNC-72-3 or HPNC-31-3) for various catalysts.

5 Conclusion

A large sum of experimental data obtained over a Pt/Al_2O_3 dehydrogenation catalyst was kinetically modeled using various Horiuti-Polanyi reaction schemes. The loss of first hydrogen atom was considered the rate-controlling step and a number of rate models were developed and tested against the data. The same kinetic model equation developed on the basis of both the Non-Competitive (HPNC) and the Combined Competitive-Non-Competitive (HPCCNC) schemes was found the best-fit model. The activation energy of 80.65 kJ/mol was obtained. The model equation suggests the presence of methylcyclohexane, toluene, and hydrogen adsorbed on active sites different to the hydrocarbon sites may possibly inhibit the rate. The best-fit model also showed the potential to fit the experimental data of various other Pt-loaded alumina catalyst.

References

[1] M. S. Akram, R. Aslam, F. S. Alhumaidan, M. R. Usman, An exclusive kinetic model for the methylcyclohexane dehydrogenation over alumina supported Pt catalysts, *Int. J. Chem. Kinet.* **52** (2020) 415–449.

[2] F. S. Alhumaidan, *Hydrogen storage in liquid organic hydrides: producing hydrogen catalytically from methylcyclohexane*, PhD, Univ. Manchester, Manchester, 2008.

[3] F. S. Alhumaidan, D. Cresswell, A. Garforth, Kinetic model of the dehydrogenation of methylcyclohexane over monometallic and bimetallic Pt catalysts, *Ind. Eng. Chem. Res.* **50** (2011) 2509–2522.

[4] T. Bera, J. W. Thybaut, G. B. Marin, Single-event microkinetics of aromatics hydrogenation on Pt/H-ZSM22, *Ind. Eng. Chem. Res.* **50** (2011) 12933–12945.

[5] C. R. Campbell, *Hydrogen storage and fuel processing strategies*, PhD, Newcastle Univ., Newcastle, 2014.

[6] A. Corma, R. Cid, L. Agudo, Catalyst decay in the kinetics of methylcyclohexane dehydrogenation over Pt-NaY zeolite, *Can. J. Chem. Eng.* **57** (1979) 638–642.

[7] J. A. Dumesic, D. F. Rudd, L. M. Aparicio, J. E. Rekoske, A. A. Treviño, *The Microkinetics of Heterogeneous Catalysis*, ACS Prof. Ref. Book, Wiley, 1993.

[8] M. El-Sawi, F. A. Infortuna, P. G. Lignola, A. Parmaliana, F. Frusteri, N. Giordano, Parameter estimation in the kinetic model of methylcyclohexane dehydrogenation on a Pt-Al2O3 catalyst by sequential experiment design, *Chem. Eng. J.* **42** (1989) 137–144.

[9] J. F. García de la Banda, A. Corma, F. V. Melo, Dehydrogenation of methylcyclohexane on a PtNaY catalyst, Study of kinetics and deactivation. *Appl. Catal.* **26** (986) 103–121.

[10] I. Horiuti, M. Polanyi, Exchange reactions of hydrogen on metallic catalysts, *Trans. Faraday Soc.* **30** (1934) 1164–1172.

[11] L. W. Jossens, E. E. Petersen, Fouling of a platinum reforming catalyst accompanying the dehydrogenation of methylcyclohexane, *J. Catal.* **73** (1982) 377–386.

[12] J. R. Kittrell, Mathematical modeling of chemical reactions, *Adv. Chem. Eng.* **8** (1970) 97–183.

[13] L. Lozano, G. B. Marin, J. W. Thybaut, Analytical rate expressions accounting for the elementary steps in benzene hydrogenation on Pt, *Ind. Eng. Chem. Res.* **56** (2017) 12953–12962.

[14] G. Maria, A. Marin, C. Wyss, S. Müller, E. Newson, Modelling and scaleup of the kinetics with deactivation of methylcyclohexane dehydrogenation for hydrogen energy storage, *Chem. Eng. Sci.* **51** (1996) 2891–2896.

[15] B. Mattson, W. Foster, J. Greimann, T. Hoette, N. Le, A. Mirich, S. Wankum, A. Cabri, C. Reichenbacher, E. Schwanke, Heterogeneous catalysis: the Horiuti–Polanyi mechanism and alkene hydrogenation, *J. Chem. Educ.* **90** (2013) 613–619.

[16] T. H. Schildhauer, E. Newson, S. Müller, The equilibrium constant for methylcyclohexane-toluene system, *J. Catal.* **198** (2001) 355–358.

[17] D. E. Tsakiris, *Catalytic production of hydrogen from liquid organic hydride*, PhD, Univ. Manchester, Manchester, 2007.

[18] M. R. Usman, Methylcyclohexane dehydrogenation over commercial 0.3wt%Pt/Al2O3 catalyst, *Proc. Pak. Acad. Sci.* **48** (2011) 13–17.

[19] M. R. Usman, D. Cresswell, A. Garforth, Detailed reaction kinetics for the dehydrogenation ofmethylcyclohexane over Pt catalyst, *Ind. Eng. Chem. Res.* **51** (2012) 158-170.

[20] P. A. Van Trimpont, G. B. Marin, G. F. Froment, Kinetics of methylcyclohexane dehydrogenation on sulfided commercial platinum/alumina and platinum-rhenium/alumina catalysts, *Ind. Eng. Chem. Fundamen.* **25** (1986) 544–553.

[21] B. Yang, X. Q. Gong, H. F. Wang, X. M. Cao, J. J. Rooney, P. Hu, Evidence to challenge the universality of the Horiuti–Polanyi mechanism for hydrogenation in heterogeneous catalysis: origin and trend of the preference of a non-Horiuti–Polanyi mechanism, *J. Am. Chem. Soc.* **135** (2013) 15244–15250.